Palmprint Recognition Using Band-Limited Minimum Average Correlation Energy Filter

Wei Jia[1], Rong-Xiang Hu[1,2], Yang Zhao[1,2], Jie Gui[1] and Yi-Hai Zhu[1,2]
[1] Hefei Institute of Intelligent Machines, CAS, Hefei, China,
[2] Department of Automation, University of Science and Technology of China
icg.jiawei@gmail.com

Abstract—**In this paper, we propose Band-Limited minimum average correlation energy filter and unconstrained minimum average correlation energy filter for palmprint recognition, in which the high frequency components are removed and only the inherent frequency band is adopted for filter design. The results of experiments conducted on Hong Kong Polytechnic University Palmprint Database show that the proposed filters can significantly improve accurate recognition rates and reduce equal error rates. Meanwhile, they also have faster matching speed and need less feature storage.**

Keywords- biometric, palmprint recognition, MACE filter, UMACE filter

I. INTRODUCTION

Nowadays, hand based biometric [1][11~18], especially palmprint recognition has been receiving wide attentions from researchers [1]. So far, there have been many approaches proposed for palmprint recognition. Kong et al. made a survey for this technique and divided the approaches into several different categories [2]. For texture based approaches, Wavelet transform, DCT, Local Binary Pattern and some statistical method are often used for texture feature extraction [2]. There are also some line based approaches since lines including principal lines and wrinkles are essential and basic features of palmprint [3]. Coding approaches are deemed to have the best performance on both accurate recognition rate and matching speed. The representative coding methods are PalmCode, FusionCode, Competitive Code, Ordinal Code, and Robust Line Orientation Code [4]. In addition, some representative appearance based approaches were also applied to palmprint recognition [5, 6, 7].

Recently, correlation methods such as optimal tradeoff synthetic discriminant function (OTSDF) filter and Band-Limited Phase-Only correlation (BL-POC) have been adopted for palmprint recognition, and low EERs were reported [8,9]. As we know, OTSDF filter can be treated as the improved version of the minimum average correlation energy (MACE) filter. Besides MACE and OTSDF filters, many other correlation filters or methods were proposed in past two decades such as unconstrained MACE (UMACE) filters, distance classifier correlation (DCCF) filter, maximum average correlation height (MACH) filter, polynomial correlation filter, optimal tradeoff circular harmonic function (OTCHF) filter, class-dependence feature analysis (CFA), and kernel correlation filters, etc [10]. These filters have been applied successfully to automatic target detection/recognition, and face recognition. Among aforementioned filters, MACE and its variant i.e. UMACE filters were widely used for real applications. However, MACE and UMACE filters might be sensitive to noise introduced from varying sources in practical applications. OTSDF filter can improve the noise tolerance degree of MACE filter by considering the output noise variance (ONV). In this paper, motivated by the work of BL-POC, we propose Band-Limited MACE (BL-MACE) and UMACE (BL-UMACE) filters, which is another effective way to improve the robustness of original MACE and UMACE filters. We also apply them to palmprint recognition. The results of experiments conducted on Hong Kong Polytechnic University (PolyU) Palmprint Database show that compared to original MACE and UMACE filters, BL-MACE and BL-UMACE filters can significantly improve accurate recognition rates and reduce equal error rates (EERs). Meanwhile, the proposed filters have faster matching speed and need less feature storage.

II. BAND-LIMITED MACE AND UMACE FILTER

A. Fundamentals of original MACE filter and UMACE filter

If we have a training set which has C classes and each class has C_p training samples, the total number of training samples is $\sum C_p$. For class p, the MACE filter design is used to synthesize a single filter template using C_p training samples. And the goal of MACE filter design is to produce correlation output plane that the value at the origin is constrained to a specific peak height (usually chosen to be 1) while minimizing correlation values at other locations. Therefore, when the filter is cross-correlated with a testing image that belongs to an authentic, the filter will exhibit sharp correlation peaks. Otherwise if the test image belongs to an imposter, the filter will output small correlation values with no discernible peak. It is well known that the MACE filter is designed in frequency domain i.e., the 2D Discrete Fourier Transforms (DFT) will be applied to training images firstly. Here, the definition of 2D DFT is given as follows:

978-1-4577-0490-1/11/$26.00 ©2011 IEEE

Given an image, $f(n_1,n_2)$, whose size is $N_1 \times N_2$, its 2D DFT i.e., $F(t_1,t_2)$ is given by:

$$F(t_1,t_2)=\sum_{n_1=0}^{N_1}\sum_{n_2=0}^{N_2} f(n_1,n_2)e^{-j2\pi(\frac{n_1t_1}{N_1}+\frac{n_2t_2}{N_2})} \quad (1)$$

Generally, the size of $F(t_1,t_2)$ is also $N_1 \times N_2$. And it should be noted that we should move the zero frequency component of $F(t_1,t_2)$ to the center of the spectrum for convenient use in matlab.

Next, we present how to generate MACE and UMACE filters. Suppose that we have C_p training images in class p, which are denoted by f_1, f_2,$\cdots$,f_{Cp} . It can be seen that each image have d pixels in it, where $d= N_1 \times N_2$. We perform 2D DFTs on these images and convert the 2D DFT arrays F_1, F_2,$\cdots$,F_{Cp} into 1-D column vectors by lexicographic ordering, which are denoted by X_1, X_2,$\cdots$,X_{Cp}, respectively. And then we define the training image data matrix X as:

$$X=[X_1, X_2, \cdots, X_{Cp}] \quad (2)$$

where the size of X is $d \times C_p$. Let the vector $\mathbf{H_{mace}}$ be the MACE filter in the frequency domain. The vector $\mathbf{H_{mace}}$ can be calculated by the following formula:

$$H_{mace} = D^{-1}X(X^{+}D^{-1}X)^{-1}u \quad (3)$$

where $D=(1/C_p)\sum_{i=1}^{C_p} D_i$, in which D_i is a diagonal matrix of size $d \times d$ whose diagonal elements are the magnitude squared of the associated element of X_i; the superscript "+" denotes conjugate transpose, and the column vector u with C_p elements contains the pre-specified correlation peak values of the training images, which are often set to 1.

UMACE, a variant of the original MACE filter, like the MACE filter minimizes the average correlation energy over a set of training images, but dose so without constraint u, thereby maximizing the peak height at the origin of the correlation plane. The UMACE filter expression $\mathbf{H_{umace}}$ is given by Equation:

$$H_{umace} = D^{-1}X \quad (4)$$

As shown, UMACE filter is not computationally intensive, especially since D is diagonal thus the inverse is easy to obtain.

B. Band-Limited MACE filter and UMACE filter

From formulas (3) and (4), we can see that all components of training samples' 2D DFT are exploited to generate MACE filter and UMACE filter. However, the 2D DFT of training sample might include meaningless components in high frequency domain. That is, the original MACE filter and UMACE filter emphasize the high frequency components, which may have less reliability. Thus, in this subsection we propose band limited MACE filter and UMACE filter by removing the high frequency components and using the inherent frequency band for filter design.

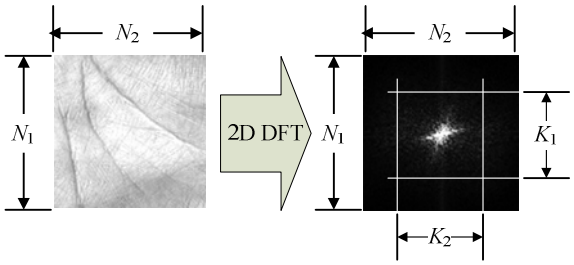

Figure 1. The K1×K2 area surrounding the center of 2D DFT spectrum is used for filter design

Given an image, $f^{(N1\times N2)}$, whose size is $N_1 \times N_2$, we can obtain its 2D DFT, $F^{(N1\times N2)}$. BL-MACE and BL-UMACE only use the components located in the center area of the spectrum for filter design as shown in Fig.1. Here we assume that the size of center area of $F^{(N1\times N2)}$ is $K_1 \times K_2$, and define this center area as $F^{(K1\times K2)}$. And then we convert the 2D DFT arrays $F_1^{(K1\times K2)}$, $F_2^{(K1\times K2)}$,$\cdots$,$F_{Cp}^{(K1\times K2)}$ into 1-D column vectors by lexicographic ordering, which are denoted by X_1^{BL}, X_2^{BL},$\cdots$,X_{Cp}^{BL}, respectively. The training image data matrix X in original MACE and UMACE should be redefined as X^{BL}:

$$X^{BL}=[X_1^{BL}, X_2^{BL}, \cdots, X_{Cp}^{BL}] \quad (5)$$

Consequently, the BL-MACE and BL-UMACE filter expressions $\mathbf{H^{BL}_{mace}}$ and $\mathbf{H^{BL}_{umace}}$ can be calculated by the following two formulas:

$$H^{BL}_{mace} = D^{BL-1}X^{BL}(X^{BL+}D^{BL-1}X^{BL})^{-1}u \quad (6)$$

$$H^{BL}_{umace} = D^{BL-1}X^{BL} \quad (7)$$

where $D^{BL}=(1/C_p)\sum_{i=1}^{C_p} D^{BL}{}_i$, in which $D^{BL}{}_i$ is a diagonal matrix of size $(K_1 \times K_2)^2$ whose diagonal elements are the magnitude squared of the associated element of X_i^{BL}. In fact, (U)MACE is the special case of BL-(U)MACE while $(K_1, K_2) = (N_1, N_2)$.

III. PERFORMANCE MEASURES

After designing $\mathbf{H^{BL}_{mace}}$ (or $\mathbf{H^{BL}_{umace}}$), we can correlate the filter with test image to produce correlation output plane as shown in Fig. 2 [10].

Suppose that $f_T^{(N1\times N2)}$ is a test image, whose size is $N_1 \times N_2$, we apply 2D DFT to it to get $F_T^{(N1\times N2)}$. And then select the center area of $F_T^{(N1\times N2)}$ to form $F_T^{(K1\times K2)}$. Also, convert the 2D DFT arrays $F_T^{(K1\times K2)}$ into 1-D column vectors by lexicographic ordering, which is denoted by X_T^{BL}. The cross-correlated vector (CV) between X_T^{BL} and H^{BL}_{mace} can be calculated by the following formula:

$$CV=IFFT((X_T^{BL})^{+} H^{BL}_{mace}) \quad (8)$$

where the *IFFT* means inverse Fourier transform. Finally, the 1D vector, CV, should be converted to 2D array by lexicographic ordering to generate the correlation output plane. Here, we define this plane as COP.

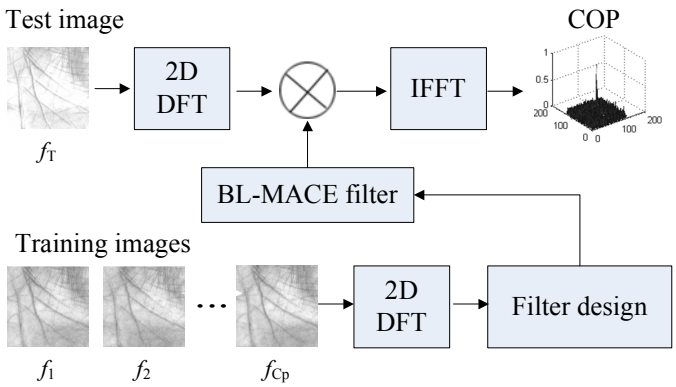

Figure 2. The framework of palmprint recognition using BL-MACE

There are some different measures to evaluate the similarity between test image and BL-MACE (or BL-UMACE) filter such as *peak*, *peak-to-correlation energy* (PCE), and *peak-to-sidelobe ratio* (PSR). As the name suggests, *peak* is the maximum peak value in the COP. PCE and PSR are defined by:

$$PCE = \frac{peak - mean_{COP}}{std_{COP}},\ PSR = \frac{peak - mean_{sidelobe}}{std_{sidelobe}} \qquad (9)$$

where $mean_{COP}$ is the average of the COP, std_{COP} is the standard deviation of the COP, $mean_{sidelobe}$ is the average of the sidelobe region surrounding the peak (21×21 pixels with a 5×5 excluded zone around the peak), and $std_{sidelobe}$ is the standard deviation of the sidelobe region values.

IV. EXPERIMENTS

The proposed approach in this paper was tested on the Hong Kong Polytechnic University (PolyU) Palmprint Database. This database contains 7752 grayscale palmprint images from 386 palms corresponding to 193 individuals, in which about 20 samples from each of these palms were collected in two sessions. And the total numbers of images captured in the first session and the second session are 3889 and 3863, respectively. A detailed introduction of PolyU Database can be found in [1]. In our paper, by using the similar preprocessing approach described in literature [1], palmprint is orientated and the ROI, whose size is 128×128, is cropped. In our experiments, we use first three palmprints from the first session for training and leave the palmprints from the second session for testing. Therefore, the numbers of images for training and test are 1158 and 3863, respectively.

The experiments were conducted on a personal computer with an Intel Duo T7500 processor (2.20GHz) and 2.0G RAM configured with Microsoft Vista and Matlab 7.0.

When designing BL-MACE and BL-UMACE filters, determining suitable values of K_1 and K_2 is a key problem that should be solved firstly. Since the ROI image of Palmprint is a square, we let K_1 equal to K_2. That is to say, the selected center area of the 2D DFT spectrum is also a square. Furthermore, in order to choose the best K_1 (or K_2), we do the tests exploiting different values of K_1 (or K_2). Here, the value of K_1 (or K_2) is set to an even number, and the range of K_1 (or K_2) is {22, 24, ···, 128}.

We firstly conducted identification experiment using 3863 test images. The nearest neighbor rule is used for classification. And the recognition rate (RR) is exploited to evaluate the identification performance. Fig. 3 depicts the RRs curves of BL-MACE (see Fig. 3a) and BL-UMACE (see Fig. 3b) using

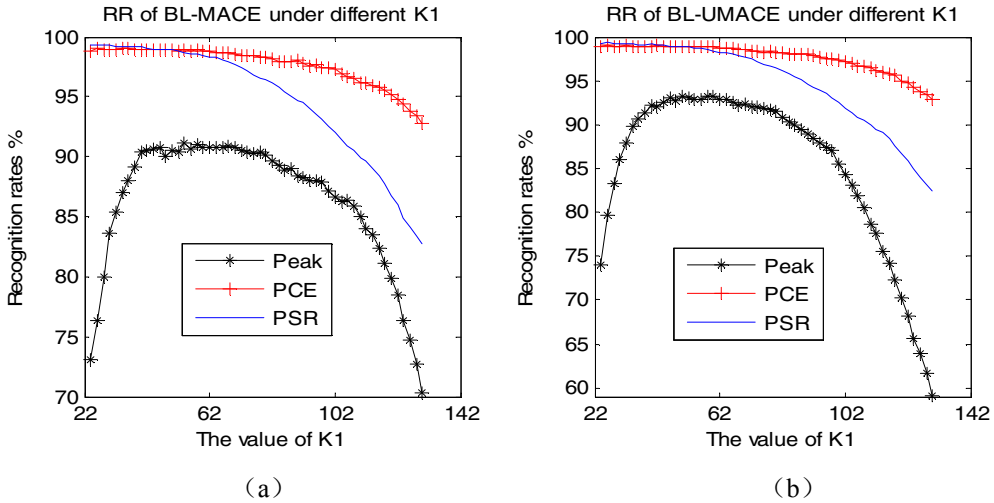

(a) (b)

Figure 3. Recognition rates (RR) of BL-MACE filter (a) and BL-UMACE filter (b) using different measures under different K1.

different measures (Peak, PCE and PSR) under different K_1.

TABLE I. THE BEST RECOGNITION RATES (BRR) OF BL-MACE AND BL-UMACE FILTERS, AND CORRESPONDING K1×K1

BL-MACE				BL-UMACE			
BRR-Peak	91.10%	$K_1 \times K_1$	52×52	BRR-Peak	93.19%	$K_1 \times K_1$	48×48
BRR-PCE	99.12%	$K_1 \times K_1$	24×24	BRR-PCE	99.07%	$K_1 \times K_1$	24×24
BRR-PSR	99.35%	$K_1 \times K_1$	28×28	BRR-PSR	99.33%	$K_1 \times K_1$	24×24

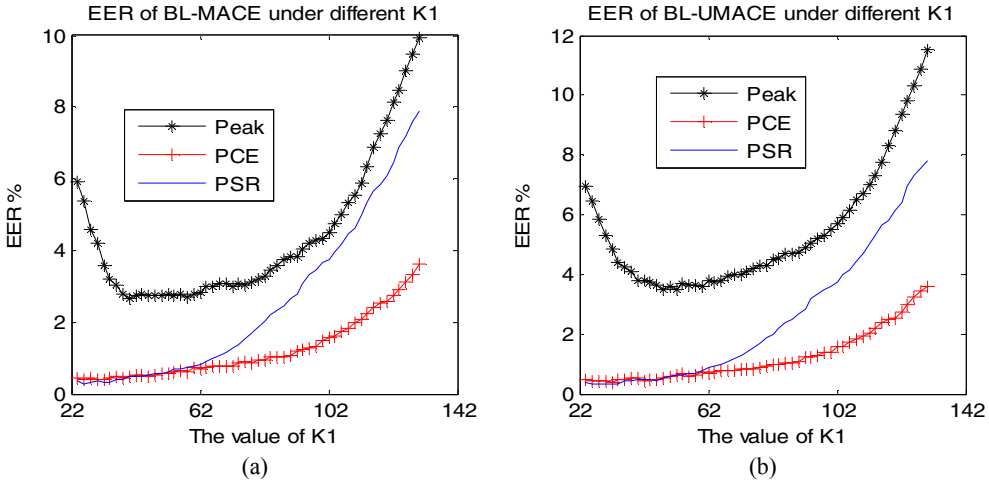

Figure 4. EERs of BL-MACE filter (a) and BL-UMACE filter (b) using different measures under different K1.

TABLE II. THE LOWEST EER (L-EER) OF BL-MACE AND BL-UMACE FILTERS USING DIFFERENT MEASURES, AND CORRESPONDING K1

BL-MACE				BL-UMACE			
L-EER-Peak	2.67%	$K_1 \times K_1$	38×38	L-EER-Peak	3.49%	$K_1 \times K_1$	50×50
L-EER-PCE	0.39%	$K_1 \times K_1$	24×24	L-EER-PCE	0.39%	$K_1 \times K_1$	30×30
L-EER-PSR	0.28%	$K_1 \times K_1$	24×24	L-EER-PSR	0.31%	$K_1 \times K_1$	24×24

TABLE III. THE RRS AND EERS OF ORIGINAL MACE AND UMACE FILTERS USING DIFFERENT MEASURES

	RR-Peak	RR-PCE	RR-PSR	EER-Peak	EER-PCE	EER-PSR
MACE	70.26%	92.80%	82.70%	9.95%	3.60%	7.90%
UMACE	59.13%	92.80	82.47%	11.50%	3.60%	7.81%

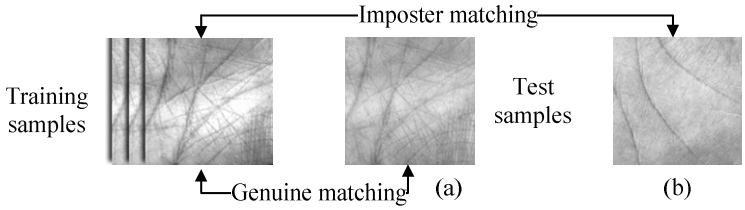

Figure 5. Genuine and imposter matching

From Fig. 3, it can be seen that when the value of K_1 changed from 128 to 22, the RRs of BL-MACE and BL-UMACE using PCE and PSR increased significantly. Table 1 shows that the best RR (BRR) of BL-MACE is 99.35% when we use PSR for performance measure and set K_1 to 28. And the BRR of BL-UMACE is 99.33% while using PSR for performance measure and setting K_1 to 24.

We secondly conducted verification experiment, and the statistical value i.e., EER, is used for performance evaluation. Fig. 4 depicts the EERs curves of BL-MACE (see Fig. 4a) and BL-UMACE (see Fig. 4b) using different measures (Peak, PCE and PSR) under different K_1. It can be seen that when the values of K_1 changed from 128 to 22, the EERs of BL-MACE and BL-UMACE using PCE and PSR reduced significantly. Table 2 shows that the lowest EER (L-EER) of BL-MACE is

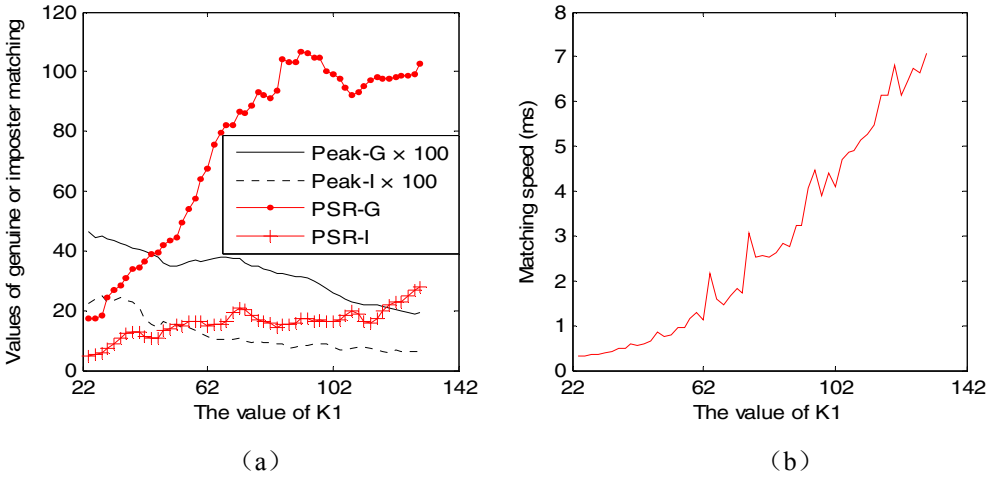

Figure 6. Trend curve of PSR and Peak values (a) and matching speed (b) when K_1 changes.

0.28% while using PSR for performance measure and setting the K_1 to 24. And the L-EER of BL-UMACE is 0.31% while using PSR and setting K_1 to 24.

Table 3 shows the RRs and EERs of original (U)MACE filter using different measures. It is easy to know that the recognition performance of (U)MACE filter is much worse than that of BL-(U)MACE filter. In order to observe the variation trend of PSR and Peak values when K_1 changes. We plot the trend curve of *Peak*-G, PSR-G (*peak* and PSR values for genuine matching) and *Peak*-I, PSR-I (*peak* and PSR values for imposter matching) as shown in Fig. 6a. The genuine and imposter matching is depicted in Fig. 5. It can be seen that when K_1 changed from 128 to 22, *peak*-G and *peak*-I increased, and PSR-G and PSR-I decreased. We also plot the trend curve of matching speed as shown in Fig. 6b. The matching speed for MACE is about 7ms, while the matching speed of BL-MACE is about 0.3ms if K_1 is set to 22.

V. CONCLUSION

In this paper, we proposed BL-MACE and BL-UMACE filters. From the experimental results, we can obtain some meaningful conclusions. Firstly, compared with original (U) MACE filter, the proposed BL-(U)MACE filter can significantly improve RRs and reduce EERs. Meanwhile, they have faster matching speed and need less feature storage. Secondly, the recognition performance of BL-UMACE nearly equals to that of BL-MACE. Thirdly, PSR is the best performance measure, and *peak* is the worst one. Finally, the best value of K_1 for palmprint recognition is at the range of {24, ···, 30}. In our future work, we will establish the relationship between BL-MACE filter and OTSDF filter, and will extend the proposed idea to other correlation filters.

ACKNOWLEDGEMENTS

This work is supported by the grants of the National Science Foundation of China, No. 61175022, 61100161, 61005010, 60705007, 60975005 and 60805021; and the grants of the Knowledge Innovation Program of the Chinese Academy of Sciences (Y023A11292 & Y023A61121).

REFERENCES

[1] D. Zhang, A. Kong, et al., "Online Palmprint Identification," IEEE T PAMI, vol. 25(9), pp. 1041-1050, 2003

[2] A. Kong, D. Zhang, M. Kamel, "A Survey of Palmprint Recognition," Pattern Recognition, vol. 42(7), pp. 1408-1418, 2009

[3] D. Huang, W. Jia, D. Zhang, "Palmprint Verification Based on Principal Lines.," Pattern Recognition, vol. 41(4), pp. 1316-1328, 2008

[4] W. Jia, D. Huang, D. Zhang, " Palmprint Verification Based on Robust Line Orientation Code," Pattern Recognition, vol. 41(5), pp. 1504-1513, 2008

[5] W. Jia, D. Huang, et al., "Palmprint Identification Based on Directional Representation," In: 2008 IEEE International Conference on SMC, Singapore, pp. 1562-1567, 2008

[6] Jie Gui, Wei Jia, Lin Zhu, Shuling Wang, Deshuang Huang, "Locality preserving discriminant projections for face and palmprint recognition," Neurocomputing, vol 73, no. 13-15, pp. 2696-2702, 2010

[7] Rongxiang Hu, Wei Jia, Deshuang Huang, Yingke Lei, "Maximum margin criterion with tensor representation," Neurocomputing, vol. 73, no.10-12, pp. 1541-1549, 2010 .

[8] P. Hennings-Yeomans, et al., "Palmprint Classification Using Multiple Advanced Correlation Filters and Palm-Specific Segmentation," IEEE T IFS, vol. 2(3),pp. 613-622, 2007

[9] K. ITO, et al., "A Palmprint Recognition Algorithm Using Phase-Only Correlation," IEICE T Fundamentals. no.4, pp.1023-1030, 2008

[10] B. Kumar, V. Savvides, C. Xie, "Correlation Pattern Recognition for Face Recognition," Proceedings of the IEEE, vol. 94(11), pp.1963-1976, 2006

[11] D. Zhang, Z.H. Guo, et al., "An online system of multispectral palmprint verification," IEEE Trans. on Instrument and Measurement, voll.59, no. 2, pp. 480-490, 2010.

[12] L. Zhang, D. Zhang,"Characterization of palmprints by wavelet signatures via directional context modeling," IEEE Trans. on System, Man and Cybernetic, Part B 34:1335-1347, 2004

[13] D. Zhang, Z.H. Guo, G.M. Lu, L. Zhang, et al., "Online joint palmprint and palmvein verification," Expert System with Applications, vol. 38, no. 3, pp. 2621-2631, 2011

[14] Z.H. Guo, W.M. Zuo, L. Zhang, D. Zhang,"A unified distance measurement for orientation coding in palmprint verification," Neurocomputing, vol. 73, pp. 944-950, 2010

[15] L. Zhang, L. Zhang, D. Zhang, H.L. Zhu,"Ensemble of local and global information for finger-knuckle-print recognition," Pattern Recognition, To appear

[16] L. Zhang, L. Zhang, D. Zhang, H. Zhu,"Online finger-knuckle-print verification for personal authentication," Pattern Recognition, vol. 3, no. 7, pp. 2560-2571, 2010

[17] Z.H. Guo, D. Zhang, L. Zhang, W.M. Zuo," Palmprint verification using binary orientation co-occurrence vector," Pattern Recognition Letters, vol. 30, no. 13, pp. 1219-1227, 2009

[18] D. Zhang, F.X. Song, Y. Xu, Z.Z. Liang, "Advanced Pattern Recognition Technologies with Applications to Biometrics", Medical Information Science Reference, 2009